Tidal cycle control of biogeochemical and ecological properties of a macrotidal ecosystem

Mathilde Cadier, Thomas Gorgues, Stéphane L'Helguen, Marc Sourisseau, Laurent Mémery

AGU PUBLICATIONS

Geophysical Research Letters

RESEARCH LETTER
10.1002/2017GL074173

Key Points:
- Numerical model resolving semidiurnal and spring/neap tidal cycles in a macrotidal ecosystem
- Spring/neap tidal cycle impacts the water column mixing and shapes the phytoplankton community in shallow waters (~100 m)
- Semidiurnal tidal cycle has a minor effect on phytoplankton and its role is modulated by the lower frequency variability (spring/neap tides)

Correspondence to:
M. Cadier,
mathilde.cadier@laposte.net

Citation:
Cadier, M., T. Gorgues, S. LHelguen, M. Sourisseau, and L. Memery (2017), Tidal cycle control of biogeochemical and ecological properties of a macrotidal ecosystem, *Geophys. Res. Lett.*, *44*, 8453–8462, doi:10.1002/2017GL074173.

Received 1 JUN 2017
Accepted 14 JUL 2017
Accepted article online 19 JUL 2017
Published online 26 AUG 2017

Tidal cycle control of biogeochemical and ecological properties of a macrotidal ecosystem

Mathilde Cadier[1], Thomas Gorgues[2], Stéphane LHelguen[1], Marc Sourisseau[3], and Laurent Memery[1]

[1]Laboratoire des Sciences de l'Environnement Marin, UMR CNRS/IFREMER/IRD/UBO 6539, Plouzané, France, [2]Laboratoire d'Océanographie Physique et Spatiale, UMR CNRS/IFREMER/IRD/UBO 6523 Ifremer, Centre de Brest, Plouzané, France, [3]Département Dynamiques de l'Environnement Côtier/PELAGOS, Ifremer Centre de Brest, Plouzané, France

Abstract In some regions, tidal energy can be a key factor in the generation of variability in physical and biogeochemical properties throughout the water column. We use a numerical model resolving tidal cycles and simulating diversity in phytoplankton to assess the impact of tidal mixing on vertical stability and phytoplankton community (total biomass and diversity) in a macrotidal sea (Iroise Sea, France). Two different time scales have been considered: semidiurnal and spring/neap tidal cycles. Our results show that the latter is the one primarily influencing the phytoplankton growth conditions by modifying the vertical stratification. During spring tide, the growth is rather light limited, whereas neap tide conditions lead to vertical stabilization and better light conditions in the shallow surface layer. The transition from high to low tidal mixing conditions is thus associated with a total phytoplankton biomass increase (caused by the rapid development of fast-growing diatoms) and reduced phytoplankton diversity.

1. Introduction

Temperate coastal ocean regions are among the most productive ecosystems on Earth [*Pauly and Christensen*, 1995; *Duarte and Cebrian*, 1996], and as such, they provide numerous ecosystem services crucial for human activities [*Barbier et al.*, 2011]. Moreover, those coastal ecosystems, lying over shallow continental shelves, are also known to be diversity hotspots with fairly complex trophic networks, which are keys in maintaining their high productivity levels and in anticipating their responses to pressures such as global warming or pollution-linked impacts [*Worm et al.*, 2006; *Loreau et al.*, 2001]. The understanding of the processes influencing the communities' composition and species diversity in those regions is therefore of great importance and represents a major challenge for marine ecologists.

The diversity of plankton species living in a single location of the ocean is known to relate to the nonresolved "paradox of the plankton" [*Hutchinson*, 1961]. Indeed, if the selection processes are driven by resources competition, the number of coexisting species should not theoretically go beyond the number of limited resources for which they compete. However, observed species diversity exceeds by far this number [*Hutchinson*, 1961]. Heterogeneity (both in time and space) of physical and biological conditions, which prevents ideal competitive exclusion, is often proposed (among other mechanisms) to explain this paradox [*Richerson et al.*, 1970; *Scheffer et al.*, 2003; *Roy and Chattopadhyay*, 2007].

Interestingly, temperate shallow waters subjected to strong turbulent movements due to tidal stirring are often seen as vertically homogeneous systems persistent over time, questioning the role of the above mentioned heterogeneity in the maintenance of their relatively high diversity. However, this assumption of shallow waters being a persistent homogeneous system may not always be true as relatively important stratification episodes can follow periods of fully mixed water column. Indeed, in those regions, variability in the water column vertical stability is mainly driven by the interactions between solar radiations (thermal stratification [*Garrett et al.*, 1978), fresh water runoffs (haline stratification [*Simpson et al.*, 1990; *Simpson and Souza*, 1995; *Ruddick et al.*, 1995]), and the intensity of vertical mixing, which depends on internal tidal mixing [*New*, 1988; *New and Pingree*, 1990; *Brickman and Loder*, 1993]. It is now well established that according to tidal oscillations, a decrease in the intensity of tidal mixing can let develop significant stratification episodes, resulting in a succession of fully mixed and stratified water column periods. In turn, the different state of vertical stability affects the physical and chemical properties of the water masses [*Webb and D'Elia*, 1980] with an impact on biological processes, including phytoplankton development [*Cullen and Lewis*, 1988;

Demers et al., 1986]. Indeed, strong vertical mixing episodes during high-energy tidal periods is (i) supplying nutrients to the surface layer by turbulent processes and diffusion through the pycnocline [*Sharples et al*., 2007], thus promoting photosynthetic growth, and (ii) transporting part of the phytoplankton below the photic layer [*Lagadeuc et al*., 1997; *Lauria et al*., 1999] with an adverse effect on growth. Conversely, during lower energy periods, a low-nutrient surface layer and only few organisms exported out of the photic layer are characterizing restratification episodes. This succession of contradictory environmental conditions is therefore most likely to influence the ecosystem structure.

Despite its potential importance in shaping the coastal communities' composition and distribution, the relationship between tidal mixing and the planktonic diversity has been rarely investigated in the past, partly due to experimental difficulties to study diversity variability at short time scales of few hours or days. In this context, emergent ecosystem models provide innovative tools to analyze the link between environmental factors (e.g., time variation of the vertical mixing) and communities' composition.

The present study is therefore aiming at quantifying the impacts of the tidal cycles on the phytoplankton community in a regional temperate macrotidal sea ecosystem. Besides its focus on an ecosystem representative of the coastal temperate ocean affected by tides, this study entails, in a rather theoretical way, the link between the high-frequency variability in environmental conditions (days to weeks) and the plankton community dynamics. Given the time scales of the phytoplankton growth (close to the high frequency investigated here), this study complements the more common studies [e.g., *Morin et al*., 1991; *Rees et al*., 1999] focusing on the seasonal variability of environmental conditions. To our knowledge, it is also the first attempt to model the direct influence of the tides on the phytoplankton diversity of a macrotidal ecosystem.

2. Methods

A regional configuration of the 3-D modeling system Regional Ocean Modeling System-Adaptive Grid Refinement In Fortran [*Shchepetkin and McWilliams*, 2005; *Debreu et al*., 2012] has been set up for the Iroise Sea ecosystem (Figure 1a; N-E Atlantic, France). The hydrodynamic model uses realistic forcing at the oceanic and ocean-atmosphere boundaries to simulate the three-dimensional ocean circulation and hydrodynamics in the Iroise Sea (from 49°30′N:06°30′W to 47°30′N;04°W) over a seasonal cycle. Despite not fully resolving the submesoscale, the 30 vertical sigma levels and the horizontal resolution of 1.5 km of our model configuration are sufficient to reproduce the main observed characteristics of the Iroise Sea with a marked tidal front [*Cadier et al*., 2017a].

An ecosystem model is then forced, online, by the 3-D circulation model (no biological feedbacks on the ocean dynamics). This ecosystem model (DARWIN model, see *Follows et al*. [2007]) simulates phytoplankton diversity represented by 120 phytoplankton types (hereafter referred as phenotypes) together with essential nutrients (nitrogen, phosphorus, and silicon), two zooplankton classes and detrital organic matter.

The phytoplankton types are evenly distributed between four functional groups: (i) diatoms (DIA), (ii) dinonanoflagellates (LND), (iii) small non-*Prochlorococcus* (SNP) including picoeukaryotes and cyanobacteria of *Synechococcus* sp. genus, and (iv) *Prochlorococcus* sp. analogs (PRO). Within each group, the 30 phenotypes are initialized with their own growth parameters (nutrient, temperature, and light affinity) stochastically chosen from a range of possible value depending on their functional group. Those stochastic choices are then realized again in the course of the simulation only to replace individual phenotypes that become extinct within the simulated region. A constant number of phenotypes are thus simulated over the full course of the modeling exercise.

The DIA and LND groups represent large phytoplankton with the highest maximal growth rate (but the lowest-nutrient affinity with nitrate half-saturation constants ranging from 0.80 to 1.12 mmol N m^{-3}) and high light optimum (mean value of 400 W m^{-2}) when compared to the SNP and PRO groups that are composed by small phytoplanktonic organisms having higher-nutrient affinity (0.24–0.56 mmol N m^{-3}) and low light optimum (215 W m^{-2}). A more detailed presentation of the functioning of the DARWIN ecosystem model can be found in *Follows et al*. [2007].

The model-specific setup used in this study is exactly the same that has been used in *Cadier et al*. [2017a, 2017b] to characterize the spatial variability of phytoplankton functional and phenotypic diversity at seasonal scale in the Iroise Sea. An extensive description of our regional setup and an exhaustive list of the model

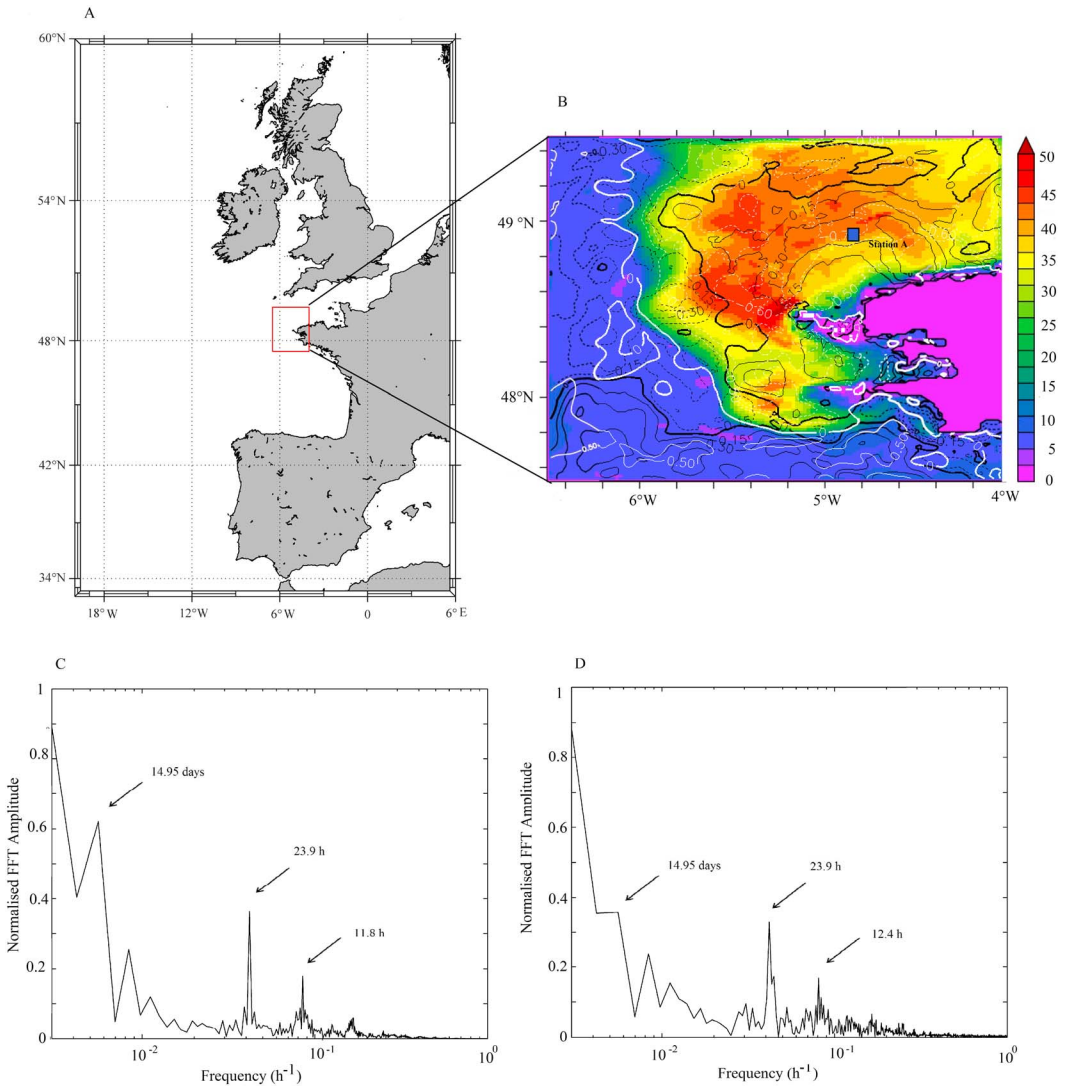

Figure 1. (a) Map of the Northeast Atlantic regional context of the study (red square: exact boundaries of our modeled area: the Iroise Sea). (b) Time standard deviation of the surface mixed-layer depth (m) during September 2007. Black lines indicate correlation coefficient between mixed-layer depth and phenotype diversity. White lines indicate correlation coefficient between mixed-layer depth and total phytoplankton concentration (mg C m^{-3}). Solid lines: positive correlation and dotted lines: negative correlation. Bold lines indicate a correlation equal to 0. (c and d) Fast Fourier transform at station A: 48°52′N–4°54′W (blue square in Figure 1b) for total phytoplankton concentration (Figure 1c) and phenotype richness (Figure 1d). The MLD standard deviation, correlations, and fast Fourier transform have been computed on averaged outputs every 30 min (1–30 September 2007).

parameters are available in those previous open access publications and have therefore not been repeated here for clarity and conciseness.

Finally, tidal forcing is performed using 15 tidal frequencies. Two of them are largely dominant in the Iroise Sea and correspond to (i) the semidiurnal cycle (also called the "M_2" tidal oscillation) with a period of 12.4 h and (ii) the spring/neap tidal cycle with a period of 14.7 days. The latter periodicity is associated to the tidal coefficient, which is defined as the quotient of the observed tidal range over the mean tidal range measured during equinoctial (strongest) spring tides at the same location. This dimensionless coefficient varies between 20 and 120. The spring tide conditions correspond to the periods during which tidal coefficients exceed 70, whereas neap tide periods are conversely characterized by lower coefficients (below 70).

In order to capture both the spring/neap tidal cycle and the semidiurnal cycle, outputs of our regional simulation have been stored with a frequency of 24 h over the summer period (June to October) and at an

additional frequency of 30 min over the month of September only (month associated with maximum seasonal stratification in the Iroise Sea) [*Mariette*, 1983]. The effect of periodic vertical tidal mixing on total phytoplankton concentration (mg C m^{-3}) and diversity (both functional diversity and phenotypes richness) is assessed for the two temporal scales. The phenotypes richness (a common measure of the diversity) is computed as the number of phenotypes whose concentration exceeds 1% of the total phytoplankton concentration. In addition, we use the Shannon Index as a complementary measure of the evenness of phenotypes within the phytoplankton community [*Pielou*, 1966; *Spellerberg and Fedor*, 2003].

3. Results

3.1. Tidal Effect on Vertical Stability, Phytoplankton Biomass, and Total Diversity

The temporal variability of the surface mixed-layer depth (MLD) (Figure 1b) shows distinctive patterns. The offshore area (southwest; with a bathymetry >100 m) displays substantial seasonal variability [*Simpson and Pingree*, 1978; *Schultes et al*., 2013; *Cadier et al*., 2017a] but remains permanently stratified (with no marked signal of tidal mixing on the MLD) during boreal summer with tidal mixing from deep bottom friction not being strong enough to break the stratification up to the surface. As bathymetry becomes shallower (northeast region with bathymetry comprised between 35 and 100 m), the MLD variability increases significantly due to the effect of tidal vertical mixing on the water column stability. Finally, very shallow (<30 m depth) waters near the coast, and in very dynamical regions around islands, are always vertically homogeneous and are not subjected to vertical stabilization, which is seen on the local MLD with no tides-related variability (Figure 1b). As a result, the region that exhibits the highest tidal variability of the MLD is located over the continental shelf (northeast and coastal part of the modeled domain) where the bathymetry ranges from 35 to 100 m (Figure 1b).

In order to document the tidal-related processes impacting coastal ecosystems, we chose to focus on this latter area. The station A, located at 48°52′N and 4°54′W with depth of 96 m (blue square in Figure 1b), is located in this high MLD variability area. As expected at this location, the fast Fourier transforms (Figures 1c and 1d) of the total phytoplankton concentration and of the diversity (phenotypes richness) over September show three distinctive peaks. The dominant signal has a characteristic period of ~15 days (Figures 1c and 1d) and is representative of the spring/neap tidal cycle. Next in importance is the ~24 h periodicity, which corresponds to the diurnal cycle, followed by a peak associated to the semidiurnal cycle (~12 h) for phytoplankton concentration and diversity.

Moreover, the station A also exhibits a maximum of negative correlation (computed from the averaged outputs every 30 min; Figure 1b) between MLD and phytoplankton concentration and a conversely high positive relationship between MLD and computed diversity.

3.2. Importance of Spring Versus Neap Tide Conditions

Using a 3 month simulation (July to September) with outputs every 24 h, several successive spring/neap cycles have been produced (Figure 2). Over the considered period, the highest coefficients of each spring tide are achieved, respectively, on 16 July (87), 2 August (95), 15 August (90), 30 August (106), 13 September (91), and 28 September (112) while lowest coefficients of neap tide periods correspond to 10 July (56), 24–25 July (33), 8 August (46), 22 August (28), 6 September (39), and 21 September (25).

During spring tides (red background color in Figure 2a), tidal mixing vertically homogenizes the whole water column at station A with a mixed layer extending to the bottom (black stripes in Figure 2a). In contrast, stratification periods (with the MLD not exceeding 10 m) occur during the neap tide periods (blue color in Figure 2a) with a warming of the shallow surface mixed layer as tidally induced mixing is not sufficient to break the stratification when the depth is around 100 m (station A). We note that the maximal water column stabilization occurs at the end of each neap tide period (Figure 2) and lasts a few days (~5 days) after the lowest tide coefficient (Figure 3a). In these conditions, the phytoplankton community in the surface mixed layer receives more light (Figure 2a) during a sufficiently long time (several days) to respond positively. Indeed, a doubling of the phytoplankton total concentration (from ~80 to ~160 mg C m^{-3}; Figure 2a) is simulated in the surface mixed layer between spring and neap tide periods as the water column stratified. Biomass maximum peaks (concentrations up to 160 mg C m^{-3}) occur at neap tides as stratification lasts longer and tide coefficients are the lowest (i.e., second neap tides of each month, corresponding to the Moon's first

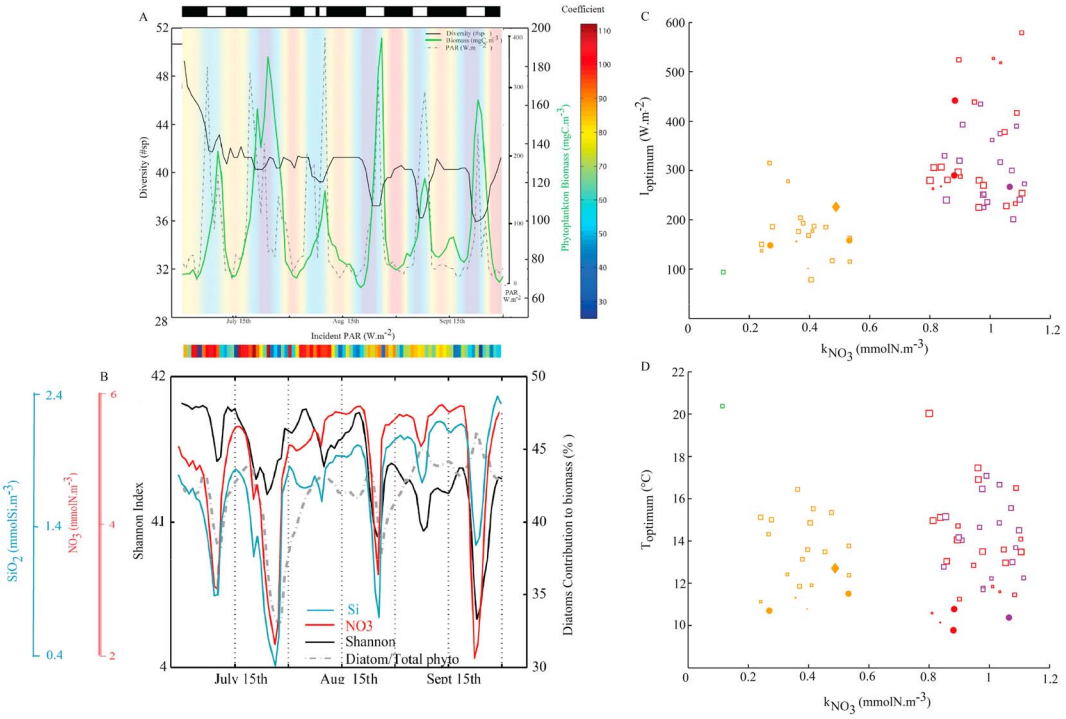

Figure 2. (a and b) Temporal evolution (averaged outputs every 24 h) of (a) available photosynthetically active radiation (W m^{-2}; dotted line), total phytoplankton concentration (mg C m^{-3}; green line), and phenotype richness (black line) and (b) Shannon Index (black line), NO_3 (mmol N m^{-3}; red line), SiO_2 (mmol Si m^{-3}; blue line), and diatom contribution to total phytoplankton concentration (%; dotted gray line) averaged over the surface mixed layer at station A between 1 July and 30 September 2007. Color on background is the tide coefficient. The top bar in Figure 2a represents the stratification of the water column: black stripes mean the whole water column is vertically homogeneous and white stripes indicate a two-layered water column with some stabilization degree. (c and d) Trait space of nitrate half-saturation constants (mmol N m^{-3}) and light optima (W m^{-2}) (Figure 2c) and temperature optima (°C) (Figure 2d) for each phytoplankton phenotype whose concentration exceeds 1% to total phytoplankton concentration at station A between 1 July and 30 September 2007. Phenotypes that are only found during spring tide time periods are represented by a circle and phenotypes only present during neap tide time periods by a diamond. Other phenotypes are represented by squares whose size is proportional to the positive difference between their concentrations during neap tide and spring tide. DIA: red, LNP: purple, SMALL: orange, and PRO: green. Spring and neap tides are defined by the surface mixed-layer depth with a threshold of 20 m deep (i.e., during neap tide periods, the MLD does not exceed 20 m (1 day average).

quarter, Figure 2a). The increase in total phytoplankton concentration corresponds to an increase in the relative contribution of larger size cells (mainly diatoms reaching 45% of the total concentration; Figures 2b–2d). By comparison with smaller phytoplankton, the diatoms exhibit the highest maximum growth rate but are less adapted to low light intensity during high mixing conditions of spring tide. Therefore, they are primarily favored by enhanced light conditions associated with the shallowing of the mixed layer during spring/neap tide transition.

At the end of the neap-tide periods, nutrients in the shallow surface mixed layer have been mainly consumed by the growing phytoplankton (as shown in Figure 2b for nitrate and silicate). As a consequence, phytoplankton growth limitation shifts from light to nutrients. The contribution of diatoms to total biomass thus eventually decreases (<40%) since silicate concentrations temporarily limit their growth. This specific situation occurs during the marked summer neap tides (tide coefficients below 35) on 24 July and 22 August (Figure 2a) when phytoplankton concentrations were maximum (Figure 2a) and silicate levels were minimum (Figure 2b). During these periods, silicate concentrations are below the diatoms' half-saturation constant for silica uptake (fixed at 1 mmol Si m^{-3} in the model) [see also *Louanchi and Najjar*, 2001]. Noticeably, nitrate concentration is not becoming a limiting factor for phytoplankton growth as nitrate concentrations are kept at significant levels (>2 mmol N m^{-3}) above the half-saturation constants.

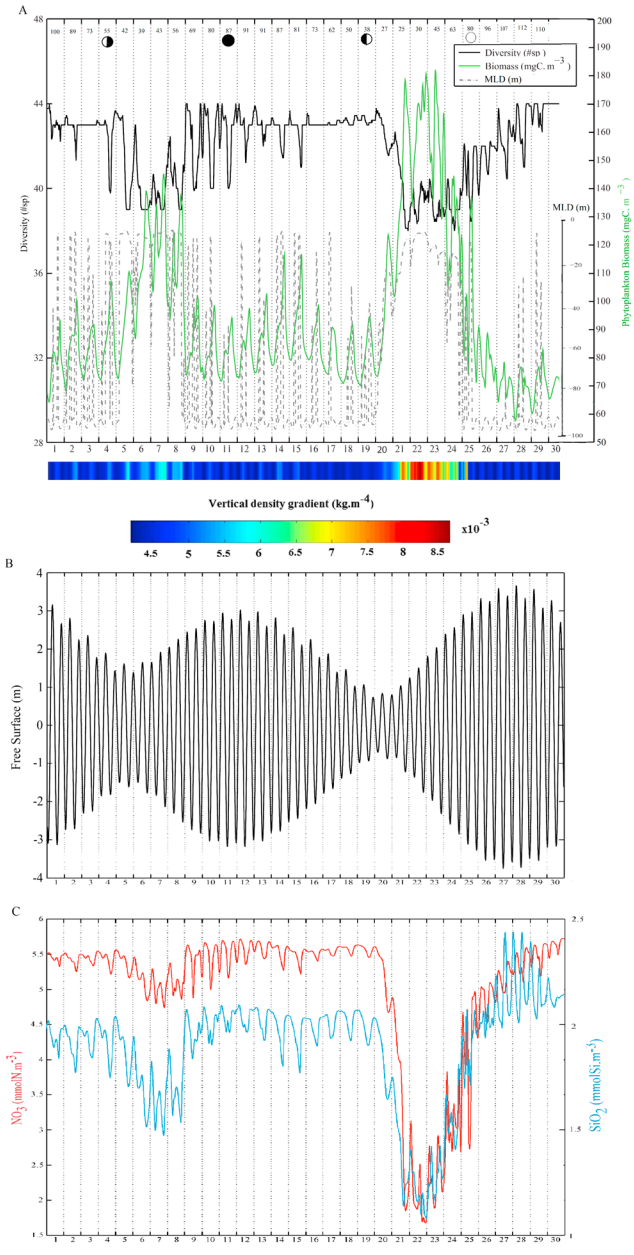

Figure 3. Temporal evolution (averaged outputs every 30 min) of (a) surface mixed-layer depth (m; dotted line), total phytoplankton concentration (mg C m^{-3}; green line), and phenotype richness (black line) averaged over the surface mixed layer; (b) free-surface (m); and (c) NO_3 (mmol N m^{-3}; red line) and SiO_2 (mmol Si m^{-3}; blue line) at station A during September 2007. Bottom bar in Figure 3a indicates the temporal evolution of the vertical density gradient (kg m^{-4}).

Given their silicate requirements, diatoms thus constitute the functional group wherein phenotypes experience the largest changes in concentration during the spring/neap tidal cycle (Figures 2c and 2d). Moreover, among the large plankton, phenotypes with the lowest light optima (below 350 W m^{-2}; Figure 3a) show the maximal variability in their concentration between spring and neap tide conditions, highlighting the substantial role of tidally driven surface mixed-layer light conditions in controlling phytoplankton growth and community composition.

The total phytoplankton increase corresponds to a decrease of both the phenotypes richness (from ~43 to ~38 phenotypes; Figure 2a) and the Shannon Index (Figure 2b) between spring and neap tide periods. This diversity decrease is explained by the selective increase of diatoms and the concurrent loss of lowest fitness phenotypes. These latter phenotypes are characterized by low temperature optima (below 12°C; Figure 2d) making them less suitable to increasingly warmer surface temperature during neap tides as we move toward the end of the summer period (Figure 2a).

3.3. Variability Due To Semidiurnal Tidal Cycle

In addition to spring/neap tide variability, the high-frequency semidiurnal tidal cycle (low/high tides whose tidal range varies according to the already described spring/neap cycle) is also likely to influence vertical stability of the water column and the phytoplankton community composition. Based on the 30 min averaged outputs, Figure 3 displays the time evolution of the MLD, the total phytoplankton concentration, and the diversity within the area of high MLD temporal variability (Figure 1b; station A: 48°52′N; 4°54′W) over September. This time period encompasses several consecutive high/low tides, which happen during three spring tide periods and two neap tide periods (Figures 3a–3c).

Our simulations show that the spring/neap tidal cycle modulates the impact of the semidiurnal tidal cycle on the water column stratification and the phytoplankton community. Focusing on the semidiurnal cycle during spring tide periods (i.e., 1–5, 9–20, and 24–30 September), one will note that some slack water (corresponding

to low tidal currents at high or low tide, see Figure 3b) are followed by a decrease in tidal barotropic currents that limits the bottom friction and let the water column stratification happen with a time lag of ~2 h (Figures 3a and 3b). Moreover, this stratification process is also modulated by the day/night cycle: the warming of the surface can only occur during day time as the incoming incident short waves radiation is sufficient while slack water that happens during nighttime leaves the water column homogeneous (mean state of the spring tide periods, Figure 3a).

The onset of a temporary stratification following slack water during daytime of spring tide periods is, however, very brief and does not exceed 1 or 2 h (2 h being most probably an overestimated value as submesoscale destratification/restratification processes are not fully resolved in our simulations). This time period is not sufficient to allow the phytoplankton community to respond significantly to the sudden increased light conditions allowed by stratification (1–5 and 10–20 September). Therefore, despite its noticeable effect on the vertical stability (diagnosed by MLD variability), the semidiurnal tidal cycle does not influence the simulated phytoplankton community, which is not able to react to the low/high tide variability of the ocean dynamics during spring tide.

The total phytoplankton concentration, which remains generally low, rather exhibits an overall diurnal cycle (Figure 3a) with an increase during daytime (~95 mg C m^{-3}) and a decrease during night time (~75 mg C m^{-3}) due to the absence of light available for photosynthesis overnight and to the direct coupling between photosynthesis and concentration change in the model.

As tidal range decreases (i.e., moving from spring to neap tide conditions), stratification becomes continuously present and constitutes the mean state during the neap tide periods (Figure 3a: 6–10 and 21–25 September). Only brief periods of enhanced vertical mixing occur and induce a slight deepening of the MLD reaching 20–60 m (depending on the tide coefficient) during short periods of time following high tides (Figure 3a), especially when high tide occurs during nighttime (i.e., in the absence of surface water warming; Figure 3b). Thus, contrary to spring tide period during which mixing is generally strong (despite short periods of relaxation during slack water), the semidiurnal tidal cycle during neap tide is not sufficient to break the permanent stratification and has a minor effect on MLD. Indeed, the computation of the phytoplankton limitation terms (varying from 0: complete limitation to 1: no limitation) during neap tides shows a nutrients limitation value of ~0.6 (Liebig's minimum law on nitrogen, phosphorus, and silicon) to be compared with a value of ~0.9 for light. Temporal variability of total phytoplankton concentrations therefore displays a more complex behavior during this neap tide period compared to spring tide conditions: an additional high-frequency variability is simulated and corresponds to the semidiurnal tidal period of 12.4 h (Figures 1a and 3a). High tides correspond to higher-nutrient and lower phytoplankton concentration in the surface mixed layer when compared to low tide conditions (Figures 3a–3c). Indeed, the slight increase of tidal mixing that follows high tide leads to a slight deepening of the shallow surface mixed layer, which in turn induce nutrients fluxes from deeper waters to the surface mixed layer and a dilution of phytoplankton concentrations (Figure 3a). A few hours after this brief episode of enhanced mixing, nutrients made available for phytoplankton growth are used in the shallow surface mixed layer and a maximum in total phytoplankton happens, associated with a consecutive nutrient depletion (Figure 3c).

As for phytoplankton concentration, high-frequency variations (12.4 h period) of the diversity (phenotypes richness) are most visible during neap tides (when compared to spring tide periods) (Figure 3a).

However, this noticeable semidiurnal related variability in phytoplankton during neap tides is much lower than the variability at lower frequency corresponding to the more contrasted spring/neap tidal cycle (concentrations change of ~40 mg C m^{-3} between high/low tides compared to ~80 mg C m^{-3} between spring/neap tides).

4. Discussion

Responses of phytoplankton growth and community composition to spring/neap cycling have been investigated by modeling [*Sharples*, 2008] and field studies [*Mcginty et al*., 2014; *Landeira et al*., 2014]. However, from our knowledge, the present study is the first in which the diversity component of phytoplankton communities is addressed in relation to tidal variability.

Using a phytoplankton trait-based model in the Iroise Sea, our results show an overall major role of spring/neap tidal cycle (period of 14.7 days, see Figures 1b–1d) in the control of the water column vertical stability over the shallow continental shelf of this macrotidal sea that, in turn, impacts both the total concentration and the phytoplankton diversity in the surface mixed layer.

During neap tides, the decline in the intensity of tidal mixing over the continental shelf allows a stratification of the water column [*Pingree et al*., 1978] that follows a period of high mixing (spring tides) and therefore provides a favorable environment for autotrophic growth with plenty of nutrients and light. In agreement with our results, *Morin et al*. [1985] observed a significant increase of chlorophyll *a* concentrations in surface waters between spring and neap tides. A relevant explanation for such variations comes from the availability of light that is the major factor controlling autotrophic growth in well-mixed coastal waters [*L'Helguen et al*., 1996; *Maguer et al*., 2011] preventing photosynthesis to occur at these latitudes when vertical mixing is strong [*Maguer et al*., 2015; *Lizon*, 2002]. Similarly, in a coastal station located on the north coast of Brittany, *Maguer et al*. [2015] have shown an overall maximum nitrogen uptake capacity and light utilization efficiency following the decrease in vertical mixing intensity at the beginning of neap tides.

The increase in total phytoplankton concentration is associated with an evenness decrease among the whole phytoplankton community (Shannon Index) and a lowering of the simulated phenotypic diversity with the loss of less adapted (low fitness) species (i.e., those with highest-temperature optimum) at the beginning of neap tides. These conditions are typical of intermittent nutrient pulses that allow phytoplankton bloom dominated by a few high-fitness species to occur in temperate ocean [*Margalef*, 1978; *Li*, 2002; *Irigoien et al*., 2004]. Indeed, the reduced mixing and reduced mixed-layer depth are more beneficial to large phytoplankton, mainly fast-growing diatoms, that are less efficient at low light levels than smaller cells. This result is in good agreement with observational data [*Brunet and Lizon*, 2003; *Maguer et al*., 2015] that also highlighted a greater contribution of large opportunistic cells as mixed-layer depth is shallowing. In the Iroise Sea, *Landeira et al*. [2014] also found an increase in the abundance of diatoms cells between spring and neap tide despite the fact that the diatom chain length is generally shorter (i.e., larger proportion of solitary cells) at neap tides in order to increase the nutrient uptake efficiency [*Pahlow et al*., 1997]. Low diversity and diatoms dominance episodes are confined to short time periods before the nutrient levels fall down progressively making nutrient the limiting factor and inducing a decrease of the diatoms proportion. This leads to a diversity recovery before the next spring tide period.

The role of semidiurnal cycle (M_2 tide) on the phytoplankton composition is least pronounced than the spring/neap tides signal and is strongly modulated by the latter lower frequency variability. Semidiurnal cycle impacts are noticeable only during the stratified periods happening at neap tide: it regulates the nutrient inputs toward the surface and the phytoplankton dilution within the stratified system. This result highlights the interactions between the different time scales of variability. Indeed, the effect of high-frequency variability (here semidiurnal period) on biogeochemical and ecological properties is thus dependent on the background state induced by lower frequency variability (i.e., here spring/neap tidal cycle).

During summer, our simulations thus show a dominant signal of the fortnightly variability (driven by the spring/neap tide cycle) leading to a temporal variation of phytoplankton diversity in the tidally impacted region of the Iroise Sea. This variability (approximately five phenotypes) is relatively low when compared to the regional spatial variability (ranging from ~35 to 50 coexisting phenotypes) [*Cadier et al*., 2017b]. Nonetheless, the fluctuations of environmental conditions (transient stratification) act as a facilitating mechanism to promote high diversity. Hence, the time-averaged seasonal richness reaches 45 phenotypes over the shallow continental shelf as a result of the coexistence over time of phenotypes with different traits values. Temporal variability is often presented as one of the explanations to the Hutchinson's paradox. It may further partly explain the larger-scale diversity patterns. Indeed, the largest diversity in the Iroise Sea is simulated in the western part of the Ushant front. A large part of the phytoplankton community is constituted by phenotypes growing in the tidally mixed waters, but several of these phenotypes are unable to locally grow within the diversity maximum itself [*Cadier et al*., 2017b]. Therefore, the tidally mixed waters region is a source of phenotypes for the broader region of the Iroise Sea. Our results highlight the role of the temporal variability of environmental conditions in (i) enhancing diversity in the tidally mixed region and (ii) maintaining the spatial patterns of high plankton diversity at regional scale through physical transport (see also *Barton et al*. [2010] for larger scale).

5. Concluding Remarks

The present study is a contribution to "how" biological diversity can be maintained in ocean through the high-frequency variability of environmental conditions. This can be of great importance considering the expected role of diversity in ecosystem resilience [*Norberg et al*., 2001; *Ptacnik et al*., 2008] toward pollution events or climate change impacts.

Here we specifically focus on the role of the tidal oscillations in shaping the phytoplankton diversity and the community composition in a shallow coastal region of a temperate macrotidal sea. Processes underlined in this study are relevant for other worldwide coastal ecosystems influenced by tides, which are among the most productive oceanic regions.

Our simulations show that the high frequency in environmental conditions induced by tides prevents an equilibrium to be reached and competitive exclusion to occur. One would think that in the absence of tidal variability, the system would have drifted toward a less diverse community as the one found at larger scale in the seasonally stratified offshore waters during the summer season [*Cadier et al*., 2017a, 2017b]. Vertical mixing induced by tides rather provides a nutrient-rich and optimal light environment (following restratification) that allows the episodic development of fast-growing, opportunist diatoms species in this part of the Iroise Sea, thus promoting species coexistence and enhancing the total diversity at seasonal scale. It is thus suggested that phytoplankton biodiversity and its link with total biomass (and productivity) depend on the considered times scales of variability and their interplay. Our study does advocate for including those kinds of interactions in global-scale studies, which do not take yet into account the high-frequency variability of the system.

Acknowledgments
This work was supported by the "Laboratoire d'Excellence" LabexMER (ANR-10-LABX-19-01) and cofunded by a grant from the French government under the program "Investissements d'Avenir" and by a grant (regional doctoral grant) from the Regional Council of Brittany. Models outputs used in this study are available at http://data.umr-lops.fr/pub/BIOTIDES/. The authors are grateful to Tristan Le Toullec and the "Laboratoire d'Oceeanographie physique et spatiale" for providing the online repository.

References

Barbier, E. B., S. D. Hacker, C. Kennedy, E. W. Koch, A. C. Stier, and B. R. Silliman (2011), The value of estuarine and coastal ecosystem services, *Ecol. Monogr.*, *81*(2), 169–193.

Barton, A. D., S. Dutkiewicz, G. Flierl, J. Bragg, and M. J. Follows (2010), Patterns of diversity in marine phytoplankton, *Science*, *327*(5972), 1509–1511.

Brickman, D., and J. W. Loder (1993), Energetics of the internal tide on northern Georges Bank, *J. Phys. Oceanogr.*, *23*(3), 409–424.

Brunet, C., and F. Lizon (2003), Tidal and diel periodicities of size-fractionated phytoplankton pigment signatures at an offshore station in the southeastern English Channel, *Estuar. Coast. Shelf Sci.*, *56*(3), 833–843.

Cadier, M., T. Gorgues, M. Sourisseau, C. A. Edwards, O. Aumont, L. Marié, and L. Memery (2017a), Assessing spatial and temporal variability of phytoplankton communities' composition in the Iroise Sea ecosystem (Brittany, France): A 3D modeling approach. Part 1: Biophysical control over plankton functional types succession and distribution, *J. Mar. Syst.*, *165*, 47–68.

Cadier, M., M. Sourisseau, T. Gorgues, C. A. Edwards, and L. Memery (2017b), Assessing spatial and temporal variability of phytoplankton communities' composition in the Iroise Sea ecosystem (Brittany, France): A 3D modeling approach: Part 2: Linking summer mesoscale distribution of phenotypic diversity to hydrodynamism, *J. Mar. Syst.*, *169*, 111–126.

Cullen, J. J., and M. R. Lewis (1988), The kinetics of algal photoadaptation in the context of vertical mixing, *J. Plankton Res.*, *10*(5), 1039–1063.

Debreu, L., P. Marchesiello, P. Penven, and G. Cambon (2012), Two-way nesting in split-explicit ocean models: Algorithms, implementation and validation, *Ocean Model.*, *49*, 1–21.

Demers, S., L. Legendre, and J. C. Therriault (1986), Phytoplankton responses to vertical tidal mixing, in *Tidal Mixing and Plankton Dynamics*, pp. 1–40, Springer, New York.

Duarte, C. M., and J. Cebrian (1996), The fate of marine autotrophic production, *Limnol. Oceanogr.*, *41*(8), 1758–1766.

Follows, M. J., S. Dutkiewicz, S. Grant, and S. W. Chisholm (2007), Emergent biogeography of microbial communities in a model ocean, *Science*, *315*(5820), 1843–1846.

Garrett, C. J. R., J. R. Keeley, and D. A. Greenberg (1978), Tidal mixing versus thermal stratification in the Bay of Fundy and Gulf of Maine, *Atmos. Ocean*, *16*(4), 403–423.

Hutchinson, G. E. (1961), The paradox of the plankton, *Am. Nat.*, *95*(882), 137–145.

Irigoien, X., J. Huisman, and R. P. Harris (2004), Global biodiversity patterns of marine phytoplankton and zooplankton, *Nature*, *429*(6994), 863–867.

Lagadeuc, Y., J. M. Brylinski, and D. Aelbrecht (1997), Temporal variability of the vertical stratification of a front in a tidal Region Of Freshwater Influence (ROFI) system, *J. Mar. Syst.*, *12*(1), 147–155.

Landeira, J. M., Ferron, B., Lunven, M., Morin, P., Marié, L., and Sourisseau, M. (2014), Biophysical interactions control the size and abundance of large phytoplankton chains at the Ushant tidal front, *PLoS One*, *9*(2), e90507.

Lauria, M. L., D. A. Purdie, and J. Sharples (1999), Contrasting phytoplankton distributions controlled by tidal turbulence in an estuary, *J. Mar. Syst.*, *21*(1), 189–197.

L'Helguen, S., C. Madec, and P. Le Corre (1996), Nitrogen uptake in permanently well-mixed temperate coastal waters, *Estuar. Coast. Shelf Sci.*, *42*(6), 803–818.

Li, W. K. W. (2002), Macroecological patterns of phytoplankton in the northwestern North Atlantic Ocean, *Nature*, *419*(6903), 154–157.

Lizon, F. (2002), Primary production in tidally mixed coastal waters: The eastern English Channel case study, *La mer*, *40*, 1–9.

Loreau, M., et al. (2001), Biodiversity and ecosystem functioning: Current knowledge and future challenges, *Science*, *294*(5543), 804–808.

Louanchi, F., and R. G. Najjar (2001), Annual cycles of nutrients and oxygen in the upper layers of the North Atlantic Ocean, *Deep-Sea Res. II*, *48*, 2155–2217.

Maguer, J. F., S. L'Helguen, J. Caradec, and C. Klein (2011), Size-dependent uptake of nitrate and ammonium as a function of light in well-mixed temperate coastal waters, *Cont. Shelf Res.*, *31*(15), 1620–1631.
Maguer, J. F., S. L'Helguen, and M. Waeles (2015), Effects of mixing-induced irradiance fluctuations on nitrogen uptake in size-fractionated coastal phytoplankton communities, *Estuar. Coast. Shelf Sci.*, *154*, 1–11.
Margalef, R. (1978), Life-forms of phytoplankton as survival alternatives in an unstable environment, *Oceanol. Acta*, *1*(4), 493–509.
Mariette, V. (1983), Effet Des Échanges Atmosphériques Sur La Structure Thermique Marine, Application À Des Zones Du Large Et Une Zone Côtière:." Thèse de doctorat, Université de Bretagne Occidentale.
Mcginty, N., M. P. Johnson, and A. M. Power (2014), Spatial mismatch between phytoplankton and zooplankton biomass at the Celtic boundary front, *J. Plankton Res.*, *36*(6), 1446–1460.
Morin, P., P. Le Corre, and J. Lefevre (1985), Assimilation and regeneration of nutrients off the west coast of Brittany, *J. Mar. Biol. Assoc. U. K.*, *65*(03), 677–695.
Morin, P., P. Le Corre, Y. Marty, and S. Lhelguen (1991), Evolution printanière des éléments nutritifs et du phytoplancton sur le plateau continental armoricain (Europe du Nord-Ouest), *Oceanol. Acta*, *14*(3), 263–279.
New, A. L. (1988), Internal tidal mixing in the Bay of Biscay. *Deep Sea Research Part A*, *Oceanogr. Res. Pap.*, *35*(5), 691–709.
New, A. L., and R. D. Pingree (1990), Evidence for internal tidal mixing near the shelf break in the Bay of Biscay, *Deep Sea Res. Part A, Oceanogr. Res. Pap.*, *37*(12), 1783–1803.
Norberg, J., D. P. Swaney, J. Dushoff, J. Lin, R. Casagrandi, and S. A. Levin (2001), Phenotypic diversity and ecosystem functioning in changing environments: A theoretical framework, *Proc. Natl. Acad. Sci.*, *98*(20), 11376–11381.
Pahlow, M., U. Riebesell, and D. A. Wolf-Gladrow (1997), Impact of cell shape and chain formation on nutrient acquisition by marine diatoms, *Limnol. Oceanogr.*, *42*, 1660–1672.
Pauly, D., and V. Christensen (1995), Primary production required to sustain global fisheries, *Nature*, *374*(6519), 255–257.
Pielou, E. C. (1966), Shannon's formula as a measure of specific diversity: Its use and misuse, *Am. Nat.*, *100*(914), 463–465.
Pingree, R. D., P. M. Holligan, and G. T. Mardell (1978), The effects of vertical stability on phytoplankton distributions in the summer on the northwest European shelf, *Deep-Sea Res.*, *25*(11), 1011–1028.
Ptacnik, R., A. G. Solimini, T. Andersen, T. Tamminen, P. Brettum, L. Lepistö, E. Willén, and S. Rekolainen (2008), Diversity predicts stability and resource use efficiency in natural phytoplankton communities, *Proc. Natl. Acad. Sci.*, *105*(13), 5134–5138.
Rees, A. P., I. Joint, and K. M. Donald (1999), Early spring bloom phytoplankton-nutrient dynamics at the Celtic Sea shelf edge, *Deep-Sea Res. I Oceanogr. Res. Pap.*, *46*(3), 483–510.
Richerson, P., R. Armstrong, and C. R. Goldman (1970), Contemporaneous disequilibrium, a new hypothesis to explain the "paradox of the plankton", *Proc. Natl. Acad. Sci.*, *67*(4), 1710–1714.
Roy, S., and J. Chattopadhyay (2007), Towards a resolution of "the paradox of the plankton": A brief overview of the proposed mechanisms, *Ecol. Complex.*, *4*(1), 26–33.
Ruddick, K. G., E. Deleersnijder, P. J. Luyten, and J. Ozer (1995), Haline stratification in the Rhine-Meuse freshwater plume: A three-dimensional model sensitivity analysis, *Cont. Shelf Res.*, *15*(13), 1597–1630.
Scheffer, M., S. Rinaldi, J. Huisman, and F. J. Weissing (2003), Why plankton communities have no equilibrium: Solutions to the paradox, *Hydrobiologia*, *491*(1), 9–18.
Sharples, J. (2008), Potential impacts of the spring-neap tidal cycle on shelf sea primary production, *J. Plankton Res.*, *30*(2), 183–197.
Sharples, J., et al. (2007), Spring-neap modulation of internal tide mixing and vertical nitrate fluxes at a shelf edge in summer, *Limnol. Oceanogr.*, *52*(5), 1735–1747.
Shchepetkin, A. F., and J. C. McWilliams (2005), The Regional Oceanic Modeling System (ROMS): A split-explicit, free-surface, topography-following-coordinate oceanic model, *Ocean Model.*, *9*(4), 347–404.
Schultes, S., M. Sourisseau, E. Le Masson, M. Lunven, and L. Marié (2013), Influence of physical forcing on mesozooplankton communities at the Ushant tidal front, *J. Mar. Syst.*, *109*, S191–S202.
Simpson, J. H., and R. D. Pingree (1978), Shallow sea fronts produced by tidal stirring, in *Oceanic Fronts in Coastal Processes*, pp. 29–42 , Springer, Berlin Heidelberg.
Simpson, J. H., J. Brown, J. Matthews, and G. Allen (1990), Tidal straining, density currents, and stirring in the control of estuarine stratification, *Estuar. Coasts*, *13*(2), 125–132.
Simpson, J., and A. Souza (1995), Semidiurnal switching of stratification in the region of freshwater influence of the Rhine, *J. Geophys. Res.*, *100*, 7037–7044.
Spellerberg, I. F., and P. J. Fedor (2003), A tribute to Claude Shannon (1916–2001) and a plea for more rigorous use of species richness, species diversity and the "Shannon–Wiener" index, *Glob. Ecol. Biogeogr.*, *12*(3), 177–179.
Webb, K. L., and C. F. D'Elia (1980), Nutrient and oxygen redistribution during a spring neap tidal cycle in a temperate estuary, *Science*, *207*(4434), 983–985.
Worm, B., et al. (2006), Impacts of biodiversity loss on ocean ecosystem services, *Science*, *314*(5800), 787–790.